

PACS numbers: 78.60.Kn, 87.50.cm, 87.50.sj, 87.50.up, 87.50.wj, 87.53.Bn, 87.57.uq

Pre- and Post-Irradiation Annealing for TLD 600 and 700 Dosimeters; Comparison of the Properties of TL Glow Peaks 5 and 5a

Mokhtar Halimi¹, Dahane Kadri², and Abdelmalek Mokeddem³

¹*Université Ahmed Ben Bella d'Oran 1,
Faculté de Médecine d'Oran, Département de Médecine,
BP 1524, El-M'Naouer, 31000, Oran, Algérie*

²*Université des Sciences et de la Technologie d'Oran Mohamed-Boudiaf,
Faculté de Physique, Département de Technologie des Matériaux,
BP 1505, El-M'Naouer, Bir El Djir, 31000, Oran, Algérie*

³*Université des Sciences et de la Technologie d'Oran Mohamed-Boudiaf,
Faculté de Physique, Département de Physique Energétique,
BP 1505, El-M'Naouer, Bir El Djir, 31000, Oran, Algérie*

LiF:Mg,Ti has found a wide spread application in artificial-phosphor dosimetric methods of thermoluminescence (TL). The pre- and post-irradiation annealing is an essential factor for materials response. The main outcome of this study is focused on studying the low-temperature pre- and post-irradiation annealings of the ⁶LiF (Harshaw TLD 600) and comparing them with those of the ⁷LiF (Harshaw TLD 700), as well as the corresponding consequences on the 5 and 5a peak trapping parameters. We selected TLD 600 and TLD 700 dosimeters to evaluate the effect of pre-irradiation and post-irradiation background measurements; readout values indicated variation of the results for these two cases of the lithium-fluoride family of materials.

LiF:Mg,Ti знайшов широке поширення застосування в штучно-фосфорних дозиметричних методах термолюмінесценції (TL). Відпал до та після опромінення є важливим чинником реакції матеріалів. Основний результат цього дослідження зосереджений на вивченні низькотемпературних відпалів до та після опромінення ⁶LiF (Harshaw TLD 600) і порівнянні їх з параметрами ⁷LiF (Harshaw TLD 700), а також відповідними наслідками для параметрів пікового захоплення 5 і 5a. Ми відібрали фтористо-літійові термолюмінесцентні дозиметри TLD 600 і TLD 700 для оцінки ефекту фонових мірянь попереднього опромінення та пост-опромінення; значення зчитування вказували на зміну результатів для цих двох випадків літій-фторидного сімейства матеріалів.

Key words: thermoluminescence, TLD 600, TLD 700, activation energy, peak 5a, peak 5.

Ключові слова: термолюмінесценція, фтористо-літійові термолюмінесцентні дозиметри TLD 600 і TLD 700, енергія активації, пік 5a, пік 5.

(Received 17 June, 2020)

1. INTRODUCTION

Lithium fluoride (LiF) material doped with Magnesium and Titanium (Mg, Ti) is set to be one of the most well established passive thermoluminescence dosimeter (TLD). LiF:Mg,Ti is largely employed to study the TL effects of parameters such as supralinearity, impurity concentration, radiation damage, *etc.* [1, 5, 22, 24].

TL glow curves of lithium fluoride yield a number of overlapping TL peaks, making thus deconvolution mandatory. Even though in other luminescent dosimetric materials, such as quartz, the TL peaks are named according to their peak maximum temperature (T_{\max}); for the case of lithium fluoride, TL peaks were given the names according to the sequential arithmetic corresponding to each one. According to this terminology, kinetic parameters, such as the activation energy E , frequency factor s , and kinetic order b , for the so-called glow peak 5 of LiF:Mg,Ti have been a major topic of TL research for many years. The interest on this topic is not only limited to the fact that LiF:Mg,Ti has been extensively used as a basic TL dosimeter, but rather enhanced due to specific peculiarities related with the reported values of E , s and b as well [6, 7, 24].

Fairchild *et al.* [1], consequently after a good fit of the experimental glow curve for the case of TLD 100, suggested the existence of a glow peak 5a between the main glow peak 5 and glow peak 6. This glow peak has shown its importance in the usual glow curve, resulting after normal annealing at 400°C for 1 h and at 100°C for 2 h. Its existence was also experimentally confirmed based on numerous techniques, including deconvolution.

The selection of both ^6LiF (Harshaw TLD 600) and ^7LiF (Harshaw TLD 700) dosimeters in order to study the effect of pre-irradiation and post-irradiation annealings on the final dosimeter readout values has been an attractive research topic of interest for more than 20 years. Kitis *et al.* have initially observed the presence of glow peak 5a in TLD 700 after a rather high temperature of 125°C and an irradiation by muons [4, 8]. At low-temperature post- or pre-irradiation annealings, the same authors reported the increase of T_{\max} of glow peak 5a [3, 8, 9]. Kitis *et al.* [9] estimated that the activation energy of glow peak 5a has to be within the range 3–3.8 eV

for DTG-4 material. High E values lead to high frequency factors (10^{30} – 10^{40} s⁻¹), values even higher, comparatively speaking, than those of glow peak 5 for LiF:Mg,Ti, knowing that activation energy and frequency factor for the latter material lie within the range 2.0–2.3 eV and 10^{19} – 10^{23} s⁻¹, respectively [2, 6]. LiF:Mg,Cu,P has even higher values of $E \cong 2.5$ eV and $s \cong 10^{25}$ s⁻¹, respectively [3]. These E and s values are considered as extremely high and were characterized previously as ‘non-physical values’ [4], and they require special interpretation, since they are lying well above the 10^7 – 10^{13} s⁻¹ region adopted by Mott and Gurney [10]; however, Bohm and Sharmann [11, 12] proposed an upper limit value of $3 \cdot 10^{15}$ s⁻¹ at 27°C for s .

Various models have been proposed in order to explain the high values of trapping parameters [1, 4, 13–17]. Fairchild *et al.* [1] were likely the first who proposed that the high values of E and s result from a complex mechanism, and the obvious first-order kinetics behaviour is a particular case or an approximation of more complicated kinetics. By using a one trap–three centre model, Chen *et al.* [16] correlated the rather high activation energy not only for peak 5 but also some other TL peaks with the narrowing of peak shape consequence of a competition in the excitation as well as the heating stage. Piters *et al.* [15] attempted to explain these high values obtained for the kinetic parameters based on Randall and Wilkins model. For alternative explanations regarding these high E and s values, the readers could refer to [2, 22].

The task of defining, under which conditions glow peak 5a appears visibly isolated from both glow peaks 5 and 6, has been difficult, and the study is focused on the TLD 700. Kitis and Otto [9] have performed pre-irradiation annealing between low temperatures of 140°C and 160°C for 1 h. After establishing the temperature of 152°C as the most appropriate one, both post- and pre-irradiation annealings were performed for various time durations up to 12 h. The present study follows on directly from this latter aforementioned citation, which ends by questioning whether the same experiment could be also performed for the TLD 600 dosimetric material. The aims of the present work include the following: (a) studying the low-temperature pre- and post-irradiation annealings of the TLD 600 and compare them with those of the TLD 700 and the corresponding consequences on the 5 and 5a peak trapping parameters; (b) investigating the TL response of peak 5a, appearing after pre- and post-irradiation annealings at 145°C for various durations, for both TLD 600 and TLD 700 dosimeters; (c) properly define conditions, under which glow peak 5a appears isolated for TLD 600 and TLD 700. This present study allows a one-to-one qualitative and quantitative comparison between the glow-curve modifications in-

duced by both pre- and post-irradiation annealing. This comparison, as will be shown below, gives novel information, which leads to a self-consistent explanation of the experimental results.

2. EXPERIMENTAL SET UP AND PROCEDURE

TL measurements were performed at the Nuclear Physics Laboratory of the Physics Department, Aristotle University of Thessaloniki, Greece, using a Littlemore type 711 setup, with a P/M tube: EMI 9635QA bialkali (Sb K–Cs) and a thermocouple type: 90/10 Ni/Cr and 97/03 Ni/Al and an optical filter transmitting in the 320–440 nm range. In all cases, a beta test dose was provided by a $^{90}\text{Sr}/^{90}\text{Y}$ beta source delivering 0.3 Gy/min. TL measurements were carried out in a nitrogen insulated environment with a constant heating rate of 2°C/s up to a maximum temperature of 350°C. The glow oven was first evacuated at 10^{-1} Torr, and N_2 of high purity was left to flow during each TL measurement. The samples used in these experiments were LiF:Mg,Ti chips purchased by Harshaw Bicon (TLD 600 and TLD 700) with dimensions of 8×4×3 mm; the mass of each LiF chip is equal to 3 mg. TL chips were thoroughly cleaned to avoid any solid or liquid contamination. Chips were annealed in a furnace at 400°C for 1 h and rapidly cooled to room temperature prior to their use. Pre- and post-irradiation annealings were performed at 145°C using an automatic furnace. Annealings were systematically followed by a rapid cool down to room temperature; a metallic cup of 2 cm in diameter and of 0.7 cm in depth was used for that purpose. Both pre- and post-irradiation annealings were performed to a range of durations between 0 and 15 hours ($t_i = 0, 2, 4, 6, 8, 10$ and 14 hours). Test dose was 500 mGy.

3. EXPERIMENTAL RESULTS

3.1. Computerized Curve Deconvolution (CGCD)

Analysis of obtained experimental glow curves in the present work was performed by a Computerized Glow Curve Deconvolution procedure (CGCD) [18]. The analytical expressions for general order kinetics (termed as GOK hereafter), which have been proposed by Kitis *et al.*, were used [19–20] as follows:

$$I(T) = I_m b^{b/(b-1)} \exp\left(\frac{E}{kT}\right) \left(\frac{T - T_m}{T_m}\right) \times \left[(b-1)(1-\Delta) \left(\frac{T^2}{T_m^2}\right) \exp\left(\frac{E}{kT}\right) \left(\frac{T - T_m}{T_m}\right) + Z_m \right]^{-b/(b-1)}, \quad (1)$$

where $\Delta = 2kT/E$, $\Delta_m = 2kT_m/E$, $Z_m = 1 + (b-1)\Delta_m$, T is the tempera-

ture, T_m is the temperature at maximum TL intensity, I_m is the maximum intensity, b is kinetics order, E trap energy depth, and k the Boltzmann constant. Curve fittings were performed by means of the Microsoft Excel software package with solver utility [18]. Figure of merit (FOM) [21] was employed for adjustment and goodness of fit defining; it is expressed by the following:

$$FOM(\%) = 100 \sum_p |TL_{\text{exp}} - TL_{\text{fit}}| / \sum_p TL_{\text{fit}} . \quad (2)$$

Low value of FOM index is synonymous of a good fit; a low value of FOM is targeted when fitting is achieved by changing every glow peak set of parameters.

Whether in pre- or post-irradiation annealings, the first-order kinetics algorithm failed to fit the glow peak 5 region. This is also the case for the glow peak 5a of the TLD 600 dosimeter, while, for the TLD 700, glow peak 5a is very well described by first order of kinetics. Thus, a general order of kinetics was adapted similarly to the case of Kitis and Otto [9]. Typical examples of deconvolved glow curves are presented in Fig. 1; plots *a* and *b* present the deconvolved glow curves corresponding to pre-irradiation and post-

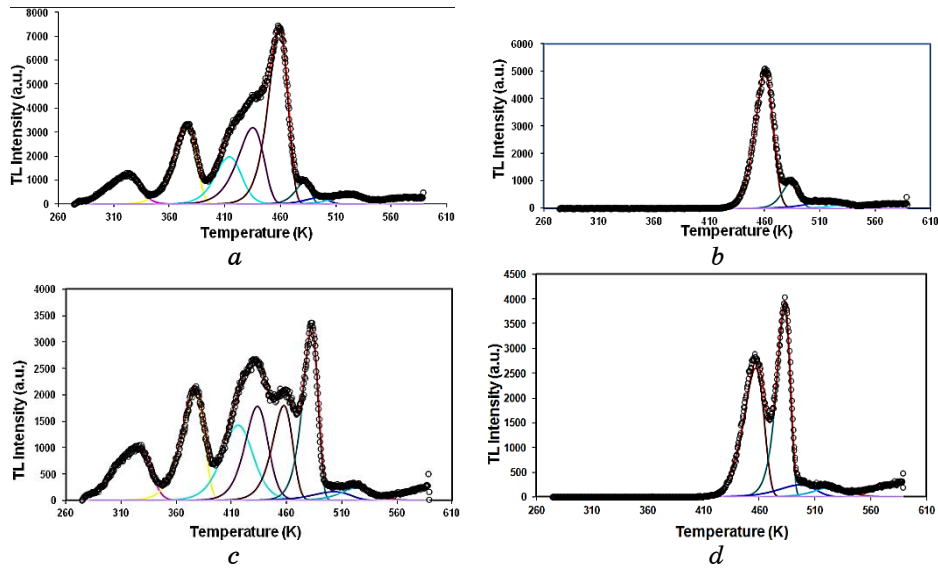


Fig. 1. Typical examples of deconvolved glow curves; plots (*a*) and (*b*) represent the deconvolved glow curves corresponding to pre-irradiation and post-irradiation annealings for 2 hours for TLD 600, respectively. Similarly, plots (*c*) and (*d*) represent the corresponding glow curves for the TLD 700.

irradiation annealings for 2 hours for TLD 600, respectively. Similarly, plots *c* and *d* present the corresponding glow curves for the TLD 700. An outline of the fitting parameters as yielded according to the deconvolution procedure is presented in tabulated form in Tables 1–4 with reference to glow peaks 5 and 5a.

TABLE 1. Fitting parameters of glow peak 5 in TLD 600 for various pre- and post-irradiation annealings' durations at 145°C.

Time	Peak 5 TLD 600					
	pre-			post-		
	E , eV	s , s ⁻¹	b	E , eV	s , s ⁻¹	b
2 h	2.21	$1.74 \cdot 10^{21}$	1.01	2.45	$1.76 \cdot 10^{25}$	1.01
4 h	1.85	$7.84 \cdot 10^{20}$	1.21	2.22	$3.08 \cdot 10^{23}$	1.10
6 h	1.78	$1.86 \cdot 10^{19}$	1.30	2.12	$1.69 \cdot 10^{22}$	1.35
8 h	1.75	$2.02 \cdot 10^{19}$	1.61	1.95	$1.73 \cdot 10^{20}$	1.52
14 h	1.74	$1.30 \cdot 10^{18}$	1.80	2.01	$4.16 \cdot 10^{19}$	1.71

TABLE 2. Fitting parameters of glow peak 5a in TLD 600 for various pre- and post-irradiation annealings' durations at 145°C.

Time	Peak 5a TLD 600					
	pre-			post-		
	E , eV	s , s ⁻¹	b	E , eV	s , s ⁻¹	b
2 h	3.11	$4.71 \cdot 10^{30}$	1.04	3.00	$6.47 \cdot 10^{29}$	1.01
4 h	3.22	$7.52 \cdot 10^{32}$	1.25	3.05	$5.85 \cdot 10^{30}$	1.14
6 h	3.28	$1.11 \cdot 10^{33}$	1.40	3.11	$1.42 \cdot 10^{31}$	1.42
8 h	3.35	$2.80 \cdot 10^{31}$	1.59	3.42	$4.61 \cdot 10^{31}$	1.55
14 h	3.43	$1.13 \cdot 10^{31}$	1.73	3.65	$5.31 \cdot 10^{30}$	1.77

TABLE 3. Fitting parameters of glow peak 5 in TLD 700 for various pre- and post-irradiation annealings' durations at 145°C.

Time	Peak 5 TLD 700					
	pre-			post-		
	E , eV	s , s ⁻¹	b	E , eV	s , s ⁻¹	b
2 h	2.15	$1.58 \cdot 10^{22}$	1.05	1.98	$1.06 \cdot 10^{21}$	1.02
4 h	1.97	$6.74 \cdot 10^{20}$	1.05	2.02	$6.18 \cdot 10^{20}$	1.11
6 h	1.90	$6.83 \cdot 10^{19}$	1.15	1.98	$7.78 \cdot 10^{20}$	1.35
8 h	1.78	$5.67 \cdot 10^{18}$	1.33	2.06	$4.19 \cdot 10^{20}$	1.44
14 h	1.85	$1.74 \cdot 10^{19}$	1.52	2.03	$1.36 \cdot 10^{21}$	1.65

TABLE 4. Fitting parameters of glow peak 5a in TLD 700 for various pre- and post-irradiation annealings' durations at 145°C.

Time	Peak 5a TLD 700					
	pre-			post-		
	E , eV	s , s ⁻¹	b	E , eV	s , s ⁻¹	b
2 h	3.03	$3.27 \cdot 10^{30}$	1.05	3.14	$1.28 \cdot 10^{34}$	1.01
4 h	3.15	$4.85 \cdot 10^{32}$	1.01	3.40	$1.47 \cdot 10^{34}$	1.01
6 h	3.15	$9.61 \cdot 10^{33}$	1.001	3.48	$1.85 \cdot 10^{33}$	1.01
8 h	3.38	$2.47 \cdot 10^{34}$	1.02	3.81	$1.87 \cdot 10^{38}$	1.01
14 h	3.63	$2.31 \cdot 10^{35}$	1.02	3.70	$3.76 \cdot 10^{38}$	1.01

3.2. Pre-Irradiation Annealing at Low Temperature

Firstly, the impact of the pre-irradiation annealing to the shape of the glow curves is presented in Figs. 2 and 3 for the case of TLD 600 and TLD 700, respectively. Figures 1, *a* and *c* show typical experimental glow curves of TLD 600 and TLD 700 both corresponding to the pre-irradiation annealing duration of 2 hours at 145°C, deconvolved into its individual TL peaks. Obtained pre-irradiation annealing glow curves made the 5a glow peak appear very distinct at 491 K; it is also interesting to note that glow peak 6 appears at the same temperature as glow peak 5a, whereas, glow peak 7 reappears at 570 K. In Figure 2, *a*, direct comparison between the TL glow-curve shapes corresponding to different annealing durations at the steady temperature of 145°C for TLD 600 is given.

According to the experimental results obtained in the present study, it was observed that the intensity of glow peak 5a decreases as annealing time increases in TLD 600. Moreover, the isolated 5a glow peak characteristics changed as pre-irradiation annealing duration changes at the temperature of 145°C. These present results confirm previous published reports detailed at Refs. [3, 8]. It is worth noticing that the intensity of the glow peak 5 decreases as a function of the annealing time. The glow peak 4 followed strongly the behaviour of glow peak 5, while a slight increase of intensity was monitored for glow peaks 1, 2 and 3.

In Figure 3, the evolution of the structure of the glow curve with respect to temperature at different durations for TLD 700 may be appreciated. Similarly to the case of TLD 600, the intensity of the glow peak 5 decreases as a function of annealing duration. The glow peak 5a appears in TLD 700 at higher annealing durations at 145°C, while the intensity of peak 5a of TLD 700 is not only very low but it is also completely distinct from glow peak 5. The intensity of the glow peak 5a decreases as a function of annealing time.

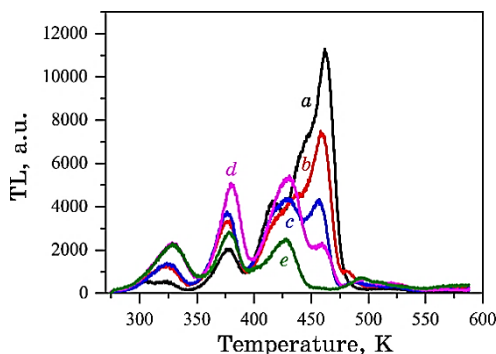


Fig. 2. Pre-irradiation annealing glow curve for TLD 600 for all temperatures: (a) 0 hour, (b) 2 hour, (c) 4 hour, (d) 8 hour, (e) 14 hour.

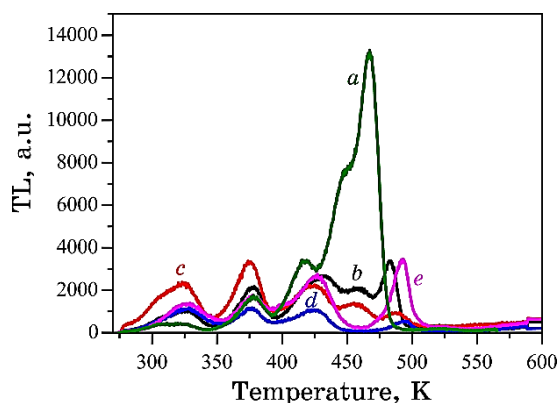


Fig. 3. Pre-irradiation annealing glow curve for TLD 700 for all temperatures: (a) 0 hour, (b) 2 hour, (c) 4 hour, (d) 8 hour, (e) 14 hour.

The intensity of the low-temperature glow peaks 1, 2 and 3 becomes more sensitive to annealing time. On the other hand, the intensity of glow peak 4 is decreased considerably for both TLD 600 and TLD 700. We can conclude that the peaks 5 and 5a yield similar behaviour for TLD 600 and TLD 700 in the pre-irradiation annealing. Nevertheless, the low-temperature pre-irradiation annealing induces a stronger variation of the glow-curve structure of the TLD 700. The peak 5a is very prominently recognized after pre-irradiation annealing for the case of the TLD 700 material, while for the TLD 600, it requires deconvolution procedure so that it could be either recognized or isolated. These figures are given in such a way that a direct comparison is possible between the pre-irradiation annealing results for both types of LiF TLDs.

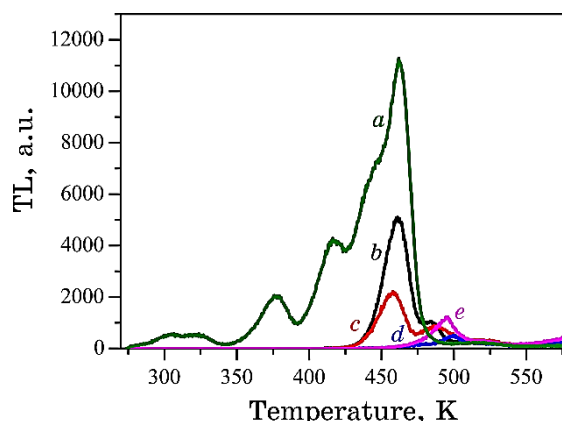


Fig. 4. Post-irradiation glow curve for TLD 600 for all temperatures: (a) 0 hour, (b) 2 hour, (c) 4 hour, (d) 8 hour, (e) 14 hour.

3.3. Low-Temperature Post-Irradiation

Figures 1, *b*, *d*, 3 and 5 present the glow curves after post-irradiation annealing at the temperature of 145°C for 2 hours. As it was stated above, in Fig. 1, *b*, the glow peak 5 was fitted using the GOK algorithm. Glow peak 5a arises as an ingredient of the high-temperature part of the main peak 5. The post-irradiation annealing at 145°C for different time durations are presented in Fig. 3, from which it can be noticed that the intensity of the glow peak 5a, isolated at this temperature, increases with annealing time. With respect to glow peak 5, its intensity decreases with post-irradiation annealing time. Glow peak 4 behaved during post-irradiation annealing in the same manner as glow peak 5, shifting to lower temperatures, while annealing time increased. In Figure 5 for TLD 700, we observe that the intensity of both glow peaks 5 and 5a decreases as a function of annealing time. The properties of peak 5a are conserved in pre- and post-irradiation annealings as in the case of TLD 700. Isolated glow peak 5a remarkably maintains its characteristics when thermally treated.

The TLD 600 glow peak 5a intensity behaviour for pre-annealing is completely different compared to its behaviour after post-irradiation, since an increase was observed in the intensity for the former case and a decrease for the latter. Once again, these observations lead us to conclude that the same mechanism is taking place during both pre- and post-irradiation annealing of TLD 700, even though [4, 17] stated that situation are not quite the same for pre- and post-irradiation annealing (empty traps for the first and captured one or more electron(s) for the second). Once again, similarly

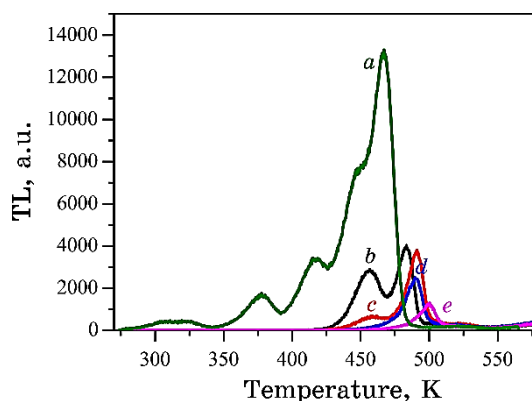


Fig. 5. Post-irradiation glow curve for TLD 700 for all temperatures: (a) 0 hour, (b) 2 hours, (c) 4 hours, (d) 8 hours, (e) 14 hours.

to the case of pre-irradiation annealing, the peak 5a is very prominently recognized after pre-irradiation annealing for the case of the TLD 700 material, while this is not the case for the TLD 600. Low-temperature pre-irradiation annealing and post-irradiation annealing similarly induce great alterations in the structure of glow peak of the TLD 700.

3.4. Pre- and Post-Irradiation Annealings' Properties at Low Temperature

In the framework of the present study, we stress our interest on glow peaks 5 and 5a, main due to the fact that T_{\max} of glow peaks 2, 3, 6 and 7 are not influenced that so ever by the conditions, under which this study was carried out. Activation energies of glow peak 5a for both TLD 600 and TLD 700 lie within the range from 3.0 to 3.7 eV for both pre- and post-irradiation annealings. Of course, these values are not high as those reported by Kitis and Otto [9] just for TLD 700. The frequency factors, being evaluated from the condition for the maximum, are extremely high in the range from 10^{29} to 10^{38} s^{-1} . The fitting parameters are presented in a tabular form in Tables 1 and 2, respectively. Similarly, for the case of the TL, glow peak 5 for both TLD 600 and TLD 700 lie within the range from 1.75 to 2.45 eV for both pre- and post-irradiation annealings, while the corresponding values of frequency factors are of the order of 10^{17} – 10^{21} s^{-1} .

The strong modification in the glow-curve structure by low-temperature pre- and post-irradiation annealings at 145°C directly affect the T_{\max} of glow peak 5a. Figures 6, a, b present T_{\max} of glow

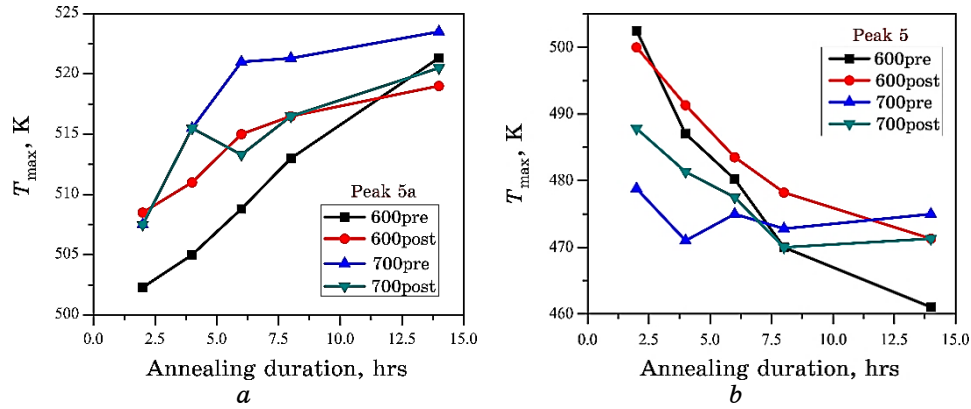


Fig. 6. Glow-peak maximum temperature T_{\max} as a function of duration of low-temperature pre/post-irradiation annealings at 145°C for ${}^6\text{LiF}$ and ${}^7\text{LiF}$: (a) glow peak 5, (b) glow peak 5a.

peaks 5a and 5 as functions of low-temperature pre- and post-irradiation annealing at 145°C for various durations, respectively. It is interesting to observe that T_{\max} of glow peak 5 is shifted towards lower temperatures. Kitis and Otto [9] reported analogous behaviour. On the other side, T_{\max} of glow peak 5a shifts towards higher temperatures. Nevertheless, in the present study, T_{\max} values are comparatively lower to those reported by Kitis and Otto for the case of TLD 600 [3, 9]. It is worth mentioning that a tendency is monitored for the case of the value obtained for the order of kinetics parameter b . In fact, as either the post- or the pre-irradiation annealing duration is increased, the kinetics parameter b obtains values, which tend to increase as well. This latter analysis feature becomes prominent according to the contents of Tables 1–4. As it was already previously mentioned, it can be easily resolved from Table 4 that glow peak 5a for the TLD 700 dosimeter is described by using first order of kinetics. We can conclude that T_{\max} of glow peak 5a of ${}^7\text{LiF}$ behave in exactly the same way for both post- and pre-irradiation annealings.

Finally, Figures 7, *a*, *b* present the dependence of the activation energy values of glow peaks 5 and 5a, respectively, as a function of the durations of low-temperature pre/post-irradiation annealings at 145°C . The behaviours versus annealing duration for TLD 600 and TLD 700 are similar, indicating a decreasing trend of both activation energy and T_{\max} versus annealing duration for the TL glow peak 5 and an inverse behaviour for both activation energy and T_{\max} versus annealing duration for the TL glow peak 5a. Finally, it should be pointed out that these behaviours for the case of TLD 700

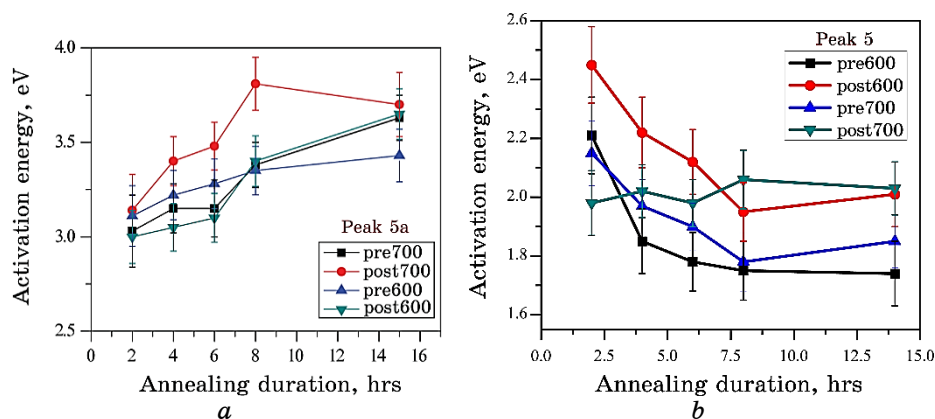


Fig. 7. The activation energy as a function of duration of low-temperature pre/post-irradiation annealings at 145°C for various durations for ⁶LiF and ⁷LiF: (a) glow peak 5a, (b) glow peak 5.

are in accordance with results reported in Ref. [9].

4. DISCUSSION

The similarities, which have been outlined above, lead to the conclusion that the same mechanism is operative during both pre- and post-irradiation annealings for both materials. This is not so obvious when we keep in mind that traps are empty at pre-irradiation annealing, whereas traps had captured one (or more) electron(s) at post-irradiation annealing [9]. Therefore, the same mechanism could be responsible for the properties of both glow peaks 5 and 5a. Nevertheless, both pre- and post-irradiation annealings at 145°C resulted in a prominent 5a TL peak for the case of TLD 700 material, while for the case of TLD 600, the peak 5a requires deconvolution analysis.

The quality, nature and curve structure of glow peak 5a could be closely linked to thermal treatment; serious modification was noticed at 145°C. From an extensive literature review [20, 22–23], where clustering and precipitation effects of the $\text{Mg}^{2+}-V_c^-$ dipoles have been studied in detail, it becomes unanimously evident that impurity–cation vacancy $\text{Mg}^{2+}-V_c^-$ dipoles and their mobility are the main causes of peaks 2 and 3; consequently, dipoles associate in clusters of two or three (dimers) dipoles. Higher order clusters of Mg^{2+} , V_c^- dipoles might be associated to peaks 4 and 5.

Serial reactions, which occur during annealing and throughout the entire temperature region, might be expressed as follow [5]:

free $\text{Mg}^{2+}-V_c^-$ + cation vacancies \rightleftharpoons dipoles \rightleftharpoons trimers \rightleftharpoons precipitates. (3)

There are some distinct temperature regions in the above reaction sequence. Below 125–130°C, the precipitation formation in very low requiring very long annealing times in order to be observed. Above 130°C, the trimers start to dissolve, whereas the precipitation formation starts showing a maximum between 140–160°C. Above 160°C, the trimers dissolve, but the precipitation formation is continuously decreased as the temperature increases up to about 250°C. Above 250°C, the formed precipitates start to dissolve, so that, above 300°C, they are completely dissolved. Therefore, above 300°C, only a few trimers can exist and almost all the Mg is in dipole form.

At 400°C, *i.e.*, at the high-temperature annealing of LiF:Mg,Ti, all the Mg is in dipole form. During the cooling to room temperature, the reaction sequence of the afore-mentioned chemical reaction is forced towards the right-hand side. The final concentrations of dipoles, trimers and precipitates at room temperature depend strongly on the cooling rate. A high sensitivity for the glow peak 5 is achieved by maximising the number of trimers and minimising the number of precipitates; this was made achievable by very fast cooling rates.

According to the above considerations, the 140–160°C region is the most effective region for precipitation formation, justifying thereby the choice of the temperature of 145°C. Another phenomena taking place in the above-mentioned temperature region is the dissociation of the $\text{Mg}^{2+}-V_c^-$ trimers and a significant reduction of the TL intensity of glow peak 5.

Observation of glow peak 5a appearance shows that, assuming that the TL of peak 5a is due to dissolution of precipitates, precipitation formation occurs equally and efficiently in the case where $\text{Mg}^{2+}-V_c^-$ has not captured an electron, corresponding to the pre-irradiation annealing, but also where $\text{Mg}^{2+}-V$ has captured an electron, corresponding to post-irradiation annealing.

In Figures 2–5, results are shown, where the pre-irradiation annealing intensity is less than post-irradiation annealing represent as an exception, which has to be clarified though. As was stated earlier, precipitation mechanism takes place during post-irradiation annealing; however, in the case of pre-irradiation annealing, one must bear in mind that $\text{Mg}^{2+}-V_c^-$ dipoles are held by Coulomb's forces, which are fairly modified by the captured electron [2]. The captured electron might inhibit the trimer dissociation, which may explain why the post-irradiation intensity is higher than the pre-irradiation.

According to the above discussion, the following mechanisms are

acting during post-irradiation annealing. (I) The typical TL decay according to first-order kinetics; (II) the dissociation of trimers with two pathways, namely, (a) a recombination from some of the $\text{Mg}^{2+}\text{-V}_c^-$ dipoles, *i.e.*, to TL emission, and (b) a precipitation, *i.e.*, to TL emission loss; (III) precipitation of the trimers with other free $\text{Mg}^{2+}\text{-V}_c^-$ dipoles, *i.e.*, to TL emission loss again. It must be noticed that the cases I and IIa are considered here as different sources of TL light emission. However, only the case IIa might exist as it is discussed below about the origin of the glow peak 5. The precipitation pathway leads to TL light loss. Consequently, the TL light obtained during the readout after a post-irradiation annealing procedure is lower than that expected due to the test dose, but still higher than the pre-irradiation annealing.

High E and s values can be considered as characteristics of the main glow peak 5 of LiF:Mg,Ti . Details and models' explanations of high E and s values are extensively reviewed in Refs. [2, 4, 17]. We dealt throughout this work essentially with glow peak 5a, which has even higher E and s values than previously mentioned ones. Results acquired from the present work show that glow peak 5a and glow peak 5 are closely linked. We can then safely conclude that the mechanism, which takes place, when high E and s values are recorded, cannot be identical for both cases.

It was even assumed that high E values of both glow peaks 5 and 5a are not real values, but apparent ones (E_{app}) [16, 17]. Decreased glow peak $FWHM$ was related to an artificial narrowing [15]. Therefore and due to the inverse relation between E and $FWHM$, the E_{app} will be larger than the expected one. Furthermore, due to the high value of E_{app} , an irregular high value of the frequency factor is also derived. McKeever [22] fully adopted the concept of high E_{app} of both glow peaks; nonetheless, Kitis and Otto [9] brought minor modifications and elementary formulation to the concept. According to the afore-mentioned citations, the activation energy of peak 5 could be expressed as the sum of the trimer binding energy (0.89 eV) and a second term related to the release of charge from the dissociated dipoles.

These extremely high values of the fitting parameters for glow peak 5a require an explanation. According to McKeever [22], peak 5 appears exactly in the range where both trimer dissociation and precipitate dissolution are taking place. This stands as a very convenient concept; however, as low-temperature pre- and post-irradiation annealings' time increases, T_{max} of glow peak 5 diminishes, whereas T_{max} of glow peak 5a increases, as in Ref. [9]. In other words, T_{max} of glow peak 5 slips towards temperatures where the dissociation becomes weaker and T_{max} of glow peak 5a moves to temperatures where the dissociation or precipitation dissolution be-

comes faster. When the T_{\max} of glow peak 5 goes to lower temperature, the E_{app} of glow peak 5 is decreased because dissociation is weaker, thus, the artificial narrowing is weak too. When T_{\max} of glow peak 5a shifts to higher temperatures, where the dissociation and the precipitation dissolution becomes very fast, the artificial narrowing is substantially increased and the E_{app} of glow peak 5a takes exaggerated high values [3, 9].

It is interesting to note that the properties of glow peak 5a are the same for both pre- and post-irradiation annealings at 145°C. This also means that, since the TL of peak 5a is attributed to the dissolution of precipitates, the precipitation formation is expected to be equally efficient in both pre-irradiation annealing ($\text{Mg}^{2+}\text{-V}$ dipoles, which have not captured an electron) and post-irradiation annealing ($\text{Mg}^{2+}\text{-V}$ dipoles, which had captured an electron). Nevertheless, the appearance of the glow peak 5a is more prominent for the case of TLD 700, while its corresponding properties, namely, E and s values, are a bit higher for the TLD 700 when compared to the corresponding values of TLD 600. This difference could be attributed to the different temperature dependence of the equilibrium states of chemical reaction (3). As it was previously stated, above 130°C, the trimers start to dissolve, whereas the precipitation formation starts showing a maximum between 140 and 160°C. This latter statement is true for the case of TLD 700, while for the case of TLD 600 material, this maximum yielded on the precipitates' formation is some shifted towards higher temperatures with a threshold temperature higher than 145°C. This is the reason, why annealing at 145°C is not so efficient in isolating glow peak 5a for TLD 600.

5. CONCLUSIONS

The conclusions from the present work are summarized as follow.

- Peaks 5 and 5a yield similar behaviour for TLD 600 and TLD 700 in the pre-irradiation annealing.
- Glow peaks 5 and 5a react for TLD 700 in the same manner in both pre- and post-irradiation annealings.
- The behaviour of peak 5a for TLD 600 is completely different at post-irradiation annealing.
- Activation energy value of glow peaks 5a for both TLD 600 and TLD 700 is within the range of 3–3.7 eV for both pre- and post-irradiation annealings.
- The frequency factors of the peak 5a are extremely high in the range of $10^{29}\text{--}10^{38} \text{ s}^{-1}$.
- The TL glow peak 5 for both TLD 600 and TLD 700 lies within the range of 1.75–2.45 eV for both pre- and post-irradiation anneal-

ings, while the corresponding values of frequency factors are of the order of 10^{17} – 10^{21} s^{-1} .

— The low-temperature post- and pre-irradiation annealings at 145°C directly affect the T_{max} of glow peak 5a.

It is important to note that the glow peak 5a appeared after a special thermal treatment in both TLD 600 and TLD 700; its characteristics are quite different from those of its neighbouring peaks 5, 6 and 7. We were able throughout this work to isolate this peak in pre- and post-irradiation processes.

REFERENCES

1. R. G. Fairchild, P. L. Mattern, K. Longweiler, and P. W. Levy, *J. Appl. Phys.*, **49**: 4523 (1978); <https://doi.org/10.1063/1.325461>
2. S. W. S. McKeever, *Thermoluminescence in Solids* (Cambridge: Cambridge University Press: 1985).
3. G. Kitis, A. Tzima, G. G. Cai, and C. Furetta, *J. Phys. D*, **29**: 1601 (1996); <https://doi.org/10.1088/0022-3727/29/6/028>
4. R. Chen and S. W. S. McKeever, *Theory of Thermoluminescence and Related Phenomena* (Singapore: World Scientific: 1997); <https://doi.org/10.1142/2781>
5. A. J. L. Bos, R. N. M. Vijverberg, T. M. Piters, and S. W. S. McKeever, *J. Phys. D*, **25**: 1249 (1992); <https://doi.org/10.1088/0022-3727/25/8/016>
6. D. Yossian and Y. S. Horowitz, *J. Phys. D*, **28**: 1495 (1995); <https://doi.org/10.1088/0022-3727/28/7/031>
7. Y. S. Horowitz and D. Yossian, *Radiation Protection Dosimetry*, **60**, Iss. 1: 3 (1995); <https://doi.org/10.1093/oxfordjournals.rpd.a082702>
8. G. Kitis and C. Furetta, *Nucl. Instrum. Methods. B*, **94**: 441 (1994); [https://doi.org/10.1016/0168-583X\(94\)95421-6](https://doi.org/10.1016/0168-583X(94)95421-6)
9. G. Kitis and T. Otto, *Nucl. Instrum. Methods. B*, **160**: 262 (2000); [https://doi.org/10.1016/S0168-583X\(99\)00589-3](https://doi.org/10.1016/S0168-583X(99)00589-3)
10. N. F. Mott and R. W. Gurney, *Electronic Processes in Ionic Crystals* (London: Oxford University Press: 1948).
11. M. Bohm, O. Erb, and A. Sharmann, *Appl. Phys. A*, **37**: 165 (1985); <https://doi.org/10.1007/BF00617501>
12. M. Bohm and A. Sharmann, *Appl. Phys. A*, **43**: 29 (1987); <https://doi.org/10.1007/BF00615202>
13. P. D. Townsend, G. C. Taylor, and M. C. Wintersgill, *Radiat. Effects*, **41**: (1979); <https://doi.org/10.1080/00337577908237933>
14. A. J. J. Bos, T. M. Piters, W. De. Vries, and J. E. Hoogenboom, *Radiation Protection Dosimetry*, **33**: 7 (1990); <https://doi.org/10.1093/oxfordjournals.rpd.a080744>
15. T. M. Piters and A. J. J. Bos, *J. Phys. D*, **26**: 2255 (1993); <https://doi.org/10.1088/0022-3727/26/12/025>
16. R. Chen and A. Hag-Yahya, *Radiat. Meas.*, **29**: 205 (1997); [https://doi.org/10.1016/S1350-4487\(96\)00147-3](https://doi.org/10.1016/S1350-4487(96)00147-3)
17. S. W. S. McKeever, M. Moscovitch, and P. D. Townsend, *Thermoluminescence Dosimetry Materials: Properties and Uses* (Ashford, Kent, England:

- Nuclear Technology Publishing: 1995).
18. D. Afouxenidis, G. S. Polymeris, N. C. T. Sirliganis, and G. Kitis, *Radiation Protection Dosimetry*, **149**, No. 4: 363 (2012); <https://doi.org/10.1093/rpd/ncr315>
 19. G. Kitis, J. M. Gomes-Ros, and J. W. N. Tuyn, *J. Phys. D*, **31**: 2636 (1998); <https://doi.org/10.1088/0022-3727/31/19/037>
 20. G. Kitis and J. M. Gomes-Ros, *Nucl. Instrum. Methods. A*, **440**: 224 (2000); [https://doi.org/10.1016/S0168-9002\(99\)00876-1](https://doi.org/10.1016/S0168-9002(99)00876-1)
 21. H. G. Balian and N. W. Eddy, *Nucl. Instrum. Methods.*, **145**: 389 (1977); [https://doi.org/10.1016/0029-554X\(77\)90437-2](https://doi.org/10.1016/0029-554X(77)90437-2)
 22. S. W. S. McKeever, *Radiation Protection Dosimetry*, **6**: 49 (1984); <https://doi.org/10.1093/oxfordjournals.rpd.a082863>
 23. G. C. Taylor and E. Lilley, *J. Phys. D*, **15**: 1243 (1982); <https://doi.org/10.1088/0022-3727/15/7/018>
 24. M. Halimi, D. Kadri, and A. Mokeddem, *Mod. Phys. Lett. B*, **29**: 1550226 (2015); <https://doi.org/10.1142/S0217984915502267>